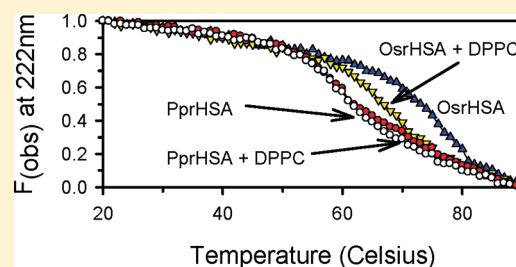


Investigation of the Differences in Thermal Stability of Two Recombinant Human Serum Albumins with 1,2-Dipalmitoyl-*sn*-glycero-3-phosphocholine Liposomes by UV Circular Dichroism Spectropolarimetry

Grant E. Frahm, Terry D. Cyr, Daryl G. S. Smith, Lisa D. Walrond, and Michael J. W. Johnston*

Centre for Vaccine Evaluation, Biologics and Genetic Therapies Directorate, Health Canada, 251 Sir Frederick Banting Driveway, Ottawa, ON K1A 0K9, Canada

ABSTRACT: Previous studies have demonstrated that liposome–protein interactions can result in changes to the thermal stability of the protein. We utilized far-UV circular dichroism spectropolarimetry and fluorescence spectroscopy to investigate the interaction of 1,2-dipalmitoyl-*sn*-glycero-3-phosphocholine (DPPC) liposomes with two recombinant human serum albumins (rHSA). We demonstrate that rHSA expressed in *Oryza sativa* (OsrHSA) has improved secondary structure thermal stability compared to rHSA expressed in *Pichia pastoris* (PprHSA). A similar stability profile was observed when comparing bovine serum albumin (BSA) and defatted bovine serum albumin (dfBSA), suggesting the presence of fatty acids may be responsible for the improved stability of OsrHSA. Addition of DPPC liposomes reduced the thermal stability of both OsrHSA and BSA, but not of PprHSA or dfBSA. DPPC liposomes may disrupt stabilizing native fatty acids on OsrHSA and BSA.



INTRODUCTION

Liposomes are nanoparticles composed of a lipid bilayer surrounding an aqueous interior and have been widely used as a drug delivery system for small molecule and genetic drugs.^{1,2} In addition to delivery systems, liposomes have also been proposed as protein excipients³ and biolubricants for synovial joints.⁴ The use of liposomes in a variety of biomedical fields has led to the extensive study of liposome–protein interactions.⁵ These interactions play critical roles in circulation lifetimes⁶ and drug release rates⁷ of nanoparticles. One protein that has been extensively studied, with respect to its interaction with liposomes, is albumin.^{5,8–10}

Albumin is the most abundant plasma transport protein and is of great importance to the pharmaceutical industry. It has been used as an excipient¹¹ and a nanoscale drug delivery system,¹² and has shown potential therapeutic utility on its own.¹³ Both bovine serum albumin (BSA) and human serum albumin (HSA) have been used interchangeably to study interactions between albumin and nanoparticles due to their high sequence homology (approximately 80%) and similar, predominately α -helical, secondary structure.¹⁴ Previous studies have shown a reduction in thermal stability of BSA in the presence of 1,2-dimyristoyl-*sn*-glycero-3-phosphocholine (DMPC) lipid nanoparticles,⁵ whereas Pantusa et al. demonstrated a 0.9 °C increase in defatted HSA stability in the presence of 1,2-dipalmitoyl-*sn*-glycero-3-phosphocholine (DPPC) liposomes using similar techniques.⁹ Thermal stability is considered an indication of protein folding, and improved conformational stability of therapeutic enzymes, cytokines, and antibodies can correlate to increased efficacy and/or half-life *in*

vivo.^{15–18} Recent studies have also shown that cationic lipids can dramatically alter the secondary structure of both BSA and HSA.^{19,20}

Considering the apparent inconsistency in the effects of phosphatidylcholines on the thermal stability of HSA and the recent development of recombinant HSA from nonanimal sources for medical purposes,²¹ it is pertinent to compare the thermal stability of rHSA expressed in *Pichia pastoris* (yeast) and *Oryza sativa* (Asian rice) in the presence of DPPC liposomes. Of interest are the potential post-translational modifications, especially in plant-based expression systems,²² which may alter liposome–protein interactions and ultimately the stability of the protein. In this study, we utilize far-UV circular dichroism spectropolarimetry to assess the structure and thermal stability of rHSA in the presence of DPPC liposomes.

EXPERIMENTAL METHODS

Materials. 1,2-Dipalmitoyl-*sn*-glycero-3-phosphocholine (DPPC) was obtained from Avanti Polar Lipids (Alabaster, AL) and used without further purification. Bovine serum albumin (BSA, $\geq 95\%$ purity, A2058: Lot 097k0741), defatted BSA (dfBSA, 100% purity, A0281: Lot 020M74001V), recombinant human serum albumin (rHSA) expressed in *P. pastoris* (PprHSA, 99% purity, A7736: Lot 080M1580V) or *O. sativa* (OsrHSA, 99% purity, A9731: Lot 120M1687),

Received: December 29, 2011

Revised: March 12, 2012

Published: March 16, 2012

phosphate buffer and bicinchoninic acid (BCA) assay kit were obtained from Sigma (St. Louis, MO). Previous X-ray crystallographic studies have demonstrated structural equivalence and disulfide matching of recombinant HSA expressed in these systems in comparison with human serum albumin obtained from plasma.^{23,24} Amicon Ultra 0.5 mL 3000 Da molecular weight cutoff (MWCO) centrifugal filter devices were purchased from Millipore (Billerica, MA). SYPRO Ruby protein stain was obtained from Invitrogen (Burlington, Canada) and Ready Gel Tris-HCl Precast Gels were supplied by Bio-Rad (Mississauga, Canada).

Protein Sample Preparation. Albumin samples were buffer exchanged into 5 mM NaPO₄, pH 7.4, with Amicon Ultra 0.5 mL 3000 Da MWCO centrifugal filter devices after prerinsing the filters with buffer. Protein concentrations were measured using a BCA assay kit. Protein integrity after buffer exchange was assessed with 1-D SDS-PAGE using SYPRO Ruby protein stain and a Bio-Rad Molecular Imager Gel Doc XR+ system with Quantity One 1-D analysis software (Bio-Rad, Mississauga, Canada).

Liposome Preparation. DPPC in chloroform was dried under a stream of nitrogen to form a thin film. Solvent was further removed by applying vacuum for at least 16 h. Multilamellar vesicles (MLVs) were generated by the addition of buffer (5 mM NaPO₄, pH 7.4) with vortexing until all dried lipid was resuspended. To produce unilamellar liposomes, MLVs were passed through two stacked Nuclepore polycarbonate filters with a pore size of 100 nm (10 passes) in a Northern Lipids Incorporated Lipex Extruder (Vancouver, BC, Canada) at temperatures above the phase transition of the lipid. Liposome particle size and distribution (number-weighted) were measured with a Particle Sizing Systems NICOMP 380 ZLS (Santa Barbara, CA). Samples were diluted in buffer (5 mM NaPO₄, pH 7.4) and scattering measurements were made at a 90° angle at 23 °C according to the manufacturer's instructions. Liposome sizes were determined to be between 65 and 75 nm.

Circular Dichroism Spectropolarimetry. Protein and DPPC liposomes were diluted to appropriate concentrations with buffer (5 mM NaPO₄, pH 7.4) in a 1 or 10 mm quartz cuvette (Hellma, Müllheim, Germany) at a 200:1 ratio (total lipid/protein, mol/mol) and were analyzed on a Jasco 815 spectropolarimeter (Jasco International Co., Ltd. Tokyo, Japan) equipped with a Peletier thermal control unit set to 37 °C. The instrument and thermal control unit were controlled with Spectra Manager Software, also from Jasco. Each far-UV circular dichroism spectrum for secondary structure analysis represents the average of 5 scans from 260 to 180 nm with a data pitch of 1 nm and a response time of 1 s. Spectra were corrected for buffer and/or liposome signal where appropriate. The calculation of secondary structure was conducted using Dichroweb (<http://dichroweb.cryst.bbk.ac.uk/html/home.shtml>) with the CDSSTR algorithm²⁵ with results presented as mean ± standard deviation of at least 3 separate experiments. Tertiary structural analyses were carried out in the near-UV region with samples analyzed between 250 and 320 nm with a data pitch of 1 nm and a response time of 1 s. Spectra were corrected for buffer and/or liposome signal where appropriate.

Thermal denaturation studies were carried out by monitoring CD (millidegrees) at 222 nm between 20 and 90 °C in increments of 2 °C/min. Samples were prepared in 1 mm quartz cuvettes (Hellma, Müllheim, Germany) at a 200:1 lipid to protein molar ratio. Spectra were corrected for buffer and/or

liposome signal where appropriate. Fractional (normalized) change was calculated according to previously published studies

$$F_{(\text{obs})} = [E_{\text{obs}}(T) - E_{\text{max}}]/[E_{20} - E_{\text{max}}]$$

where $E_{\text{obs}}(T)$ is the ellipticity at 222 nm at temperature T , E_{max} is the ellipticity at the maximum temperature (°C) used, and E_{20} is the ellipticity at the initial temperature of 20 °C.^{26,27}

Intact Mass Analysis. Intact mass analyses were performed on a Waters Global QTOF mass spectrometer (Waters Canada, Mississauga, ON, Canada) which was calibrated using a mixture of trypsinogen (1 pmol/μL) and leucine enkephalin (0.1 pmol/μL). Calibration checks on intact proteins were performed using ubiquitin, lysozyme, and BSA protein standards and deconvoluted masses were within ±2 Da of expected values. Samples were diluted 1:100 with injection solvent (3% acetonitrile (ACN), 0.2% formic acid (FA)) and 2 μL was loaded onto a Zorbax 300SB-C8 trap column (Agilent Technologies, 5 μm, 5 mm × 0.3 mm). The retained protein was washed with a 0.1% FA solution for 3 min at a flow rate of 5 μL/min and then eluted at 2 μL/min over a 45 min gradient from 3 to 85% ACN in 0.1% FA. Materials eluting from the column were ionized by electrospray using a capillary voltage of 2.5 kV and mass analyzed over an m/z range of 500–2500. MS scans in which protein peak series were detected were summed and deconvoluted using MaxEnt 1 (Waters Corporation) to yield intact mass measurements.

Tryptic Peptide Analysis. A 5 μL aliquot from each sample was added to 200 μL of 50 mM ammonium bicarbonate (NH₄HCO₃) followed by the addition of 10 μL of 250 mM dithiothreitol (DTT) in 50 mM NH₄HCO₃. Samples were then incubated for 1 h at 60 °C, after which 20 μL of 250 mM iodoacetamide in 50 mM NH₄HCO₃ was added to each one. Samples were incubated at room temperature in the dark for 30 min. The alkylation reactions were quenched by the addition of a further 20 μL of 250 mM DTT and the samples transferred onto 10 kDa molecular weight cutoff spin filters and centrifuged for 20 min at 14 000g. Samples were then washed with 2 × 200 μL of 50 mM NH₄HCO₃ centrifuging to near dryness between each wash at 14 000g for 20 min. Trypsin solution was prepared by adding 1000 μL of 50 mM NH₄HCO₃ to 20 μg of lyophilized protein and digestion was carried out by spinning 100 μL of trypsin solution through the filters at 10 000g over 20 min, then spinning 100 μL of 50 mM NH₄HCO₃ through the filter under the same conditions. The flow-throughs from the digestion steps were collected in clean tubes, evaporated to dryness in a vacuum centrifuge, and resuspended in 40 μL of injection solvent (3% ACN, 0.2% FA, and 0.05% TFA in water) prior to LC-MS/MS analysis.

For each sample, 2 μL aliquots were analyzed by loading onto a Waters Symmetry C18 trap column (180 μm × 20 mm with 5 μm beads) and desalting with 0.1% FA in water (solvent A) for 3 min at 5.0 μL/min before separating on a Waters nanoAcquity UPLC BEH130 C18 reverse phase analytical column (100 μm × 100 mm with 1.7 μm beads). Chromatographic separation was achieved at a flow rate of 0.5 μL/min over 70 min in six linear steps as follows (solvent B was 0.1% FA in ACN): Initial, 3% B; 2 min, 10% B; 40 min, 30% B; 50 min, 95% B; 55 min, 95% B; 56 min, 3% B; end, 3% B. The eluting peptides were analyzed by MS and MS/MS using a Waters Synapt HDMS system operating in DDA mode. MS survey scans were 1 s in duration and MS/MS data were collected on the four most abundant peaks until either the total ion count exceeded 3000 or until 3 s elapsed. Replicate analyses

of peaks within ± 600 mass to charge ratio (m/z) were permitted after a 60 s exclusion period. Peaks from singly charged peptides were excluded from selection for MS/MS analysis. The instrument was calibrated prior to sample analysis using the fragmentation products of [Glu1]-Fibrinopeptide B. Calibration accuracy was maintained throughout the analyses using a nanolock spray of 100 fmol/ μ L [Glu1]-Fibrinopeptide B, which was sampled for 1 s once every 30 s. The lock mass correction was applied to the data during processing.

Tryptic Peptide Analysis Data Processing. Data was processed using the Mascot software package, available from Matrix Science Ltd. (Boston, MA). The raw data was processed using Mascot Distiller (version 2.3.2) to create Mascot Generic Files (MGFs) and database searches were performed using Mascot (version 2.3), against the human protein entries in the 2011-05-04 SwissProt database. Peptide and MS/MS mass tolerances were 100 ppm and 0.1 Da, respectively, and tryptic peptides, having charges 2+, 3+ or 4+ and up to three missed cleavages, were considered. Carbamidomethylation was specified as a fixed modification and oxidation of methionine and hexose addition on lysine and arginine were considered as variable modifications. Mascot search results were then compared using the Scaffold software platform (version 3.2, Proteome Software, Inc., Portland, OR) with protein and peptide identification confidence limits at 99% and 80%, respectively.

Fluorescence Spectroscopy. Albumins were assayed alone or were mixed with DPPC liposomes at molar ratios between 50:1 and 800:1 (total lipid to protein) and subsequently incubated for 20 min prior to measurement. Fluorescence measurements were conducted on a Varian Cary Eclipse Fluorescence Spectrometer controlled with Cary Eclipse Scan Application software (Agilent Technologies, Mississauga, ON, Canada). Scans were conducted with an excitation wavelength of 280 nm and emission wavelengths of 300–500 nm with excitation/emission slit widths of 5 nm each. Fluorescence spectra were corrected for buffer and/or liposome signal where appropriate. The maximum tryptophan fluorescence intensity for each incubated sample was used to calculate binding constants and number of bound lipids for each albumin with methods utilized in previously published studies.^{19,20}

8-Anilino-1-naphthalene sulfonic acid (ANS) and protein were mixed at a molar ratio of 10:1 and then read on a Varian Cary Eclipse Fluorescence Spectrometer controlled with Cary Eclipse Scan Application software. Liposomes were also added at a 200:1 molar ratio (total lipid to protein), either before or after ANS was mixed with albumin. Scans were conducted with an excitation wavelength of 380 nm and emission wavelengths of 400–600 nm with excitation/emission slit widths of 5 nm each.

Statistical Analysis. Paired t test analyses for circular dichroism were carried out utilizing SigmaPlot 11.2.0.5 software. Significance was designated as $P < 0.05$.

RESULTS

Circular Dichroism Structural Analysis. Circular dichroism spectropolarimetry was used to assess both the secondary and tertiary structure of the albumins alone and in the presence of DPPC liposomes at 25 °C. Both BSA and rHSA (Figure 1A, BSA/dfBSA inset) showed spectra that are typical of proteins with a high content of α -helical secondary structure, with strong negative bands at 222 and 208 nm and a strong positive band at 190 nm. Deconvolution of the spectral data with the CDSSTR

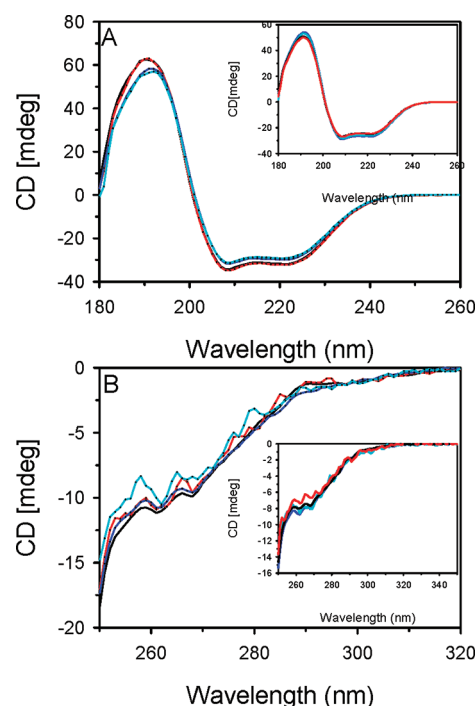


Figure 1. Far (A) and near (B) UV CD spectra for PprHSA and OsrHSA in the absence and presence of DPPC liposomes (200:1 total lipid/protein, mol/mol). CD spectra were measured on a Jasco 815 spectropolarimeter in 5 mM NaPO₄, pH 7.4. PprHSA (black), PprHSA + DPPC (red), OsrHSA (blue), and OsrHSA + DPPC (cyan). Protein concentrations for all samples were 0.15 mg/mL for far-UV CD and 0.53 mg/mL for near-UV CD. Each spectrum represents the mean of at least 3 separate experiments. Insets show BSA (blue), BSA + DPPC (cyan), dfBSA (black), and dfBSA + DPPC (red).

algorithm showed that both BSA variants had reduced α -helical content compared to the rHSA samples (Table 1) and only

Table 1. Secondary Structure Content Determined with Far-UV Circular Dichroism Spectropolarimetry for Various Serum Albumin Samples at 25 °C

	dfBSA ^a	BSA ^a	PprHSA ^a	OsrHSA ^a
Free Protein				
% Alpha helix	59.3 \pm 0.6	63.0 \pm 1.7	69.7 \pm 0.6	67.3 \pm 2.5
% Beta structure	18.0 \pm 0.0	17.0 \pm 1.0	14.0 \pm 1.7	15.7 \pm 0.6
% Unordered	22.3 \pm 0.6	21.0 \pm 0.0	17.7 \pm 1.5	18.0 \pm 1.7
With DPPC Liposomes				
% Alpha helix	59.0 \pm 0.0	62.0 \pm 1.7	70.3 \pm 0.6	65.7 \pm 1.5
% Beta structure	18.7 \pm 0.0	17.7 \pm 1.0	13.0 \pm 1.0	16.3 \pm 1.2
% Unordered	22.3 \pm 0.0	21.0 \pm 0.0	16.7 \pm 0.6	18.7 \pm 1.5

^aMean values \pm standard deviation for at least 3 separate experiments.

minor differences in secondary structure content were noted between dfBSA and BSA or between PprHSA and OsrHSA (Table 1). Near-UV CD analysis showed similar tertiary arrangements between dfBSA/BSA and PprHSA/OsrHSA (Figure 1B, BSA/dfBSA inset).

The addition of DPPC liposomes to the albumin samples at 25 °C resulted in no statistically significant differences ($P > 0.05$) in α -helical content for any albumin assayed (Figure 1A, BSA/dfBSA inset, Table 1). Near-UV CD analysis showed that DPPC liposomes affected the tertiary structure of all proteins

examined. Subtle changes were observed between wavelengths of 250 and 270 nm for dfBSA, BSA, and PprHSA (Figure 1B, BSA/dfBSA inset), suggesting subtle rearrangements of phenylalanine residues.²⁸ OsrHSA in the presence of DPPC liposomes showed dramatic changes in the near-UV CD spectrum between wavelengths of 250 and 270 nm, and at approximately 280 nm (Figure 1B). These observations suggest that the presence of DPPC liposomes results in the rearrangement of phenylalanine as well as tyrosine residues of OsrHSA.²⁸

Assessment of Thermal Stability of Secondary Structure. In addition to determining structure, far-UV CD can be used to monitor thermal stability of proteins. Because of albumin's highly α -helical structure, monitoring far-UV CD at 222 nm over a temperature range is ideal for assessing its thermal stability. Analysis of the fraction change in ellipticity at 222 nm and deconvolution of spectra collected at 70 °C showed that OsrHSA displayed enhanced retention of secondary structure compared to dfBSA, BSA, or PprHSA (Figure 2, Table 2). Remarkably, at this temperature, PprHSA lost twice as much α -helical structure (18.4%) as OsrHSA (9.6%) did (Table 2).

Thermal stability of albumin secondary structure was also assessed in the presence of DPPC liposomes (Figure 2).

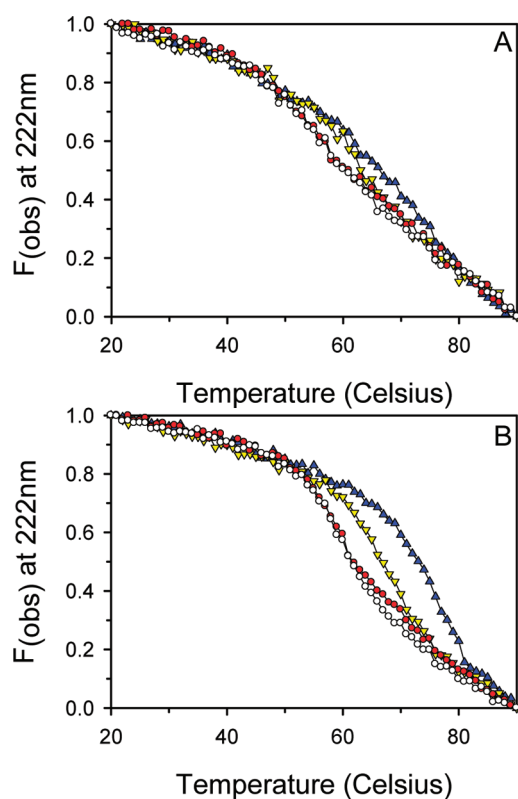


Figure 2. Fractional change in ellipticity at 222 nm (F_{obs}) with temperature for serum albumins as monitored by far-UV circular dichroism with a Jasco 815 spectropolarimeter at protein concentrations of 0.15 mg/mL. Serum albumins were assessed in the absence and presence of DPPC liposomes (200:1 total lipid/protein mol/mol) in buffer (5 mM NaPO_4 , pH 7.4). (A) BSA (blue triangles), BSA + DPPC (yellow inverted triangles), dfBSA (red circles), and dfBSA + DPPC (white circles). (B) OsrHSA (blue triangles), OsrHSA + DPPC (yellow inverted triangles), PprHSA (red circles), and PprHSA+DPPC (white circles). Each spectrum represents the mean of at least 3 separate experiments.

CDSSTR deconvolution showed no significant differences in secondary structure content of dfBSA or PprHSA in the absence or presence of DPPC liposomes at 70 °C (Figure 2, Table 2). Conversely, a significant reduction in secondary structure was seen for both BSA (4.4%, $P = 0.042$) and OsrHSA (7.2%, $P = 0.008$) in the presence of DPPC liposomes at 70 °C when compared to the free proteins at the same temperature (Figure 2, Table 2). Interestingly, the two bovine serum albumins, as well as the two human serum albumins, showed significant differences between each other ($P < 0.05$) in calculated α -helical content at 70 °C (Table 2). In the presence of DPPC liposomes, however, both BSA and OsrHSA demonstrate no significant differences in α -helical content at 70 °C compared to dfBSA ($P = 0.677$) and PprHSA ($P = 0.144$), respectively (Table 2).

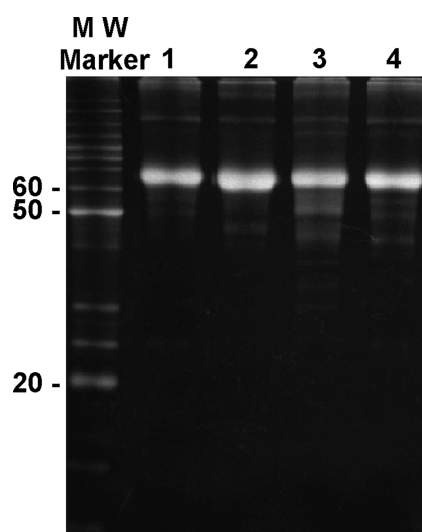
Characterization of Albumin Samples. To ascertain the basis of the observed differences in secondary structure stability, the albumin samples were further characterized with SDS-PAGE and mass spectrometry analysis. SDS-PAGE analysis of the four albumins demonstrated that BSA, dfBSA, OsrHSA, and PprHSA are of high purity with correct molecular weights (Figure 3). OsrHSA did show some smearing around the main band suggesting the possibility of post-translational modifications (Figure 3, lane 4). To confirm these results, further characterization of the four albumins was carried out with mass spectrometry. Intact mass spectra from samples of BSA, dfBSA, and PprHSA all contained well-defined series of peaks and yielded deconvoluted mass spectra showing a clear principal component within expected values (Table 3). OsrHSA however, did not generate mass spectra with well-defined peak series at initial concentration and deconvolution software was unable to clearly identify a principal component mass. The less resolved, lower intensity peak series observed for OsrHSA (Figure 4B) are typical of samples containing several isoforms or modified versions of a protein co-eluting from the UPLC. The result is overlapping peak series and diminished signal-to-noise ratios, typically making deconvolution and intact mass measurement very difficult. A second analysis of OsrHSA at 50-fold higher concentration was therefore also performed. This yielded a peak series that when smoothed, could be deconvoluted, though with a relatively low signal-to-noise ratio and potentially reduced mass accuracy (Figure 4, Table 3). In the deconvoluted mass spectrum of OsrHSA, a resolved series of peaks is observed and the one matching the expected protein mass (66439 Da) is not the most intense. This suggests that OsrHSA is more extensively modified than any of the other three. The difference between the expected mass of 66439 Da and the first major peak of 66559 Da suggests cysteinylolation,²⁹ and the mass difference between the first and second peaks (66559 and 66724 Da) in the deconvoluted spectrum is 165 Da, which is within error limits for the expected mass shift resulting from the addition of hexose.

To further confirm the presence of hexose, tryptic peptide analysis was conducted and all four albumins yielded identifications of the expected serum albumin strains with similar Mascot protein scores (~ 9000 – 10000) and protein sequence coverages (89–90%). However, the numbers of hexose-modified lysine residues identified using the noted Scaffold thresholds varied considerably, with sample OsrHSA having more than twice as many as any other sample (Table 3). On the basis of both the intact and tryptic peptide analyses, it is apparent that OsrHSA is more extensively modified than BSA, dfBSA, or PprHSA and that this can be largely attributed to an

Table 2. α -Helical Content of Serum Albumin Samples at 70 °C Determined with Far-UV Circular Dichroism Spectropolarimetry

	dfBSA ^a	BSA ^a	PprHSA ^a	OsrHSA ^a
% Alpha helix at 70 °C, free protein	43.7 \pm 3.2 ^b	48.9 \pm 0.5 ^b	51.3 \pm 0.6 ^b	57.7 \pm 2.1 ^b
% Loss of α helix at 70 °C vs 25 °C, free protein	15.6	14.1	18.4	9.6
% Alpha helix at 70 °C with DPPC liposomes	43.3 \pm 2.3	44.3 \pm 3.1	51.8 \pm 0.6	50.5 \pm 1.0
% Loss of α helix at 70 °C, DPPC liposomes vs free protein	0.4	4.6 ^c	−0.5	7.2 ^c

^aMean values \pm standard deviation for at least 3 separate experiments. ^bSignificant difference ($P < 0.05$). ^cSignificant difference at 70 °C compared to free protein ($P < 0.05$).

**Figure 3.** Twelve percent SDS–PAGE of four serum albumins. BenchMark molecular weight markers (major bands are 50 and 20 kDa). Lane 1, BSA; lane 2, PprHSA; lane 3, OsrHSA; lane 4, dfBSA.**Table 3. Summary of MS Data: Expected versus Measured (Deconvoluted) Mass of Intact Serum Albumin Samples, Mascot Protein Scores, Percent Sequence Coverage and Scaffold Identified Hexose Modified Lysine Residues for 4 Serum Albumin Samples**

sample	expected mass (Da)	measured (deconvoluted) mass (Da)	Mascot score	sequence coverage	hexose modified lysines
BSA	66432	66426	10137	90%	3
dfBSA	66432	66428	10763	90%	7
PprHSA	66306 ^a	66320	9333	89%	2
OsrHSA	66439	66559, 66724, 66883, 67044	9347	89%	17

^aPprHSA: single deletion at the N-terminus (Asp).

increase in hexose modifications on lysine residues in the OsrHSA sample relative to the other three samples.

Fluorescence Analysis. Intrinsic tryptophan fluorescence ($\lambda_{\text{ex}} = 280$ nm) was utilized to assess the tertiary structure and binding of DPPC liposomes to dfBSA, BSA, and the two rHSA samples. Structural rearrangements may result in the residue being exposed to solvent and a resultant shift in the wavelength of maximal fluorescence emission ($\lambda_{\text{em,max}}$) or a reduction in the quantum yield (fluorescence intensity) of the residue due to quenching by newly adjacent residues.³⁰ BSA showed reduced fluorescence intensity compared to dfBSA with a similar trend observed between OsrHSA and PprHSA (Figure 5, similar results were observed when $\lambda_{\text{em}} = 297$ nm (data not shown)).

The increased fluorescence intensity observed in Figure 5 for BSA/dfBSA compared to PprHSA/OsrHSA are most likely due to the presence of two tryptophan residues in BSA (Trp-134,212) and only one (Trp-214) in the recombinant HSA proteins.

In addition, OsrHSA showed a distinct blue shift in intrinsic tryptophan fluorescence $\lambda_{\text{em,max}}$ compared to the other 3 albumins examined (Figure 5, Table 4, similar results were observed when $\lambda_{\text{em}} = 297$ nm (data not shown)). This suggests the single tryptophan present in OsrHSA is buried within the protein and protected from hydrophilic environments to a greater degree than the tryptophan residue found in PprHSA. The observed reduction in intrinsic tryptophan fluorescence intensity for OsrHSA compared to PprHSA is most likely due to the presence of fatty acids, as previous research has attributed the quenching of tryptophan fluorescence (and blue shifting of $\lambda_{\text{em,max}}$) to the presence of bound fatty acids.^{19,20,31} The addition of DPPC liposomes decreased the intrinsic tryptophan fluorescence intensity for all serum albumins examined (approximately 40%) and caused no statistically significant ($P > 0.05$) shifts in $\lambda_{\text{em,max}}$ (Figure 5, Table 4).

Using varying ratios of total lipid to protein (50:1 to 800:1 mol/mol) and plotting a modified Stern–Volmer equation ($\log [(F_0 - F)/F]$ vs $\log [\text{lipid}]$, where F_0 is initial fluorescence and F is measured fluorescence in the presence of a quencher), the binding constants (K_A) and number of bound lipids (n) per albumin were estimated¹⁹ (Figure 6). All albumins showed low affinity binding for DPPC consistent with previous studies investigating lipid interactions with BSA and HSA^{19,20} and all albumins examined showed approximately 1 DPPC lipid molecule bound per albumin molecule. A single DPPC lipid molecule binding is consistent with studies identifying a fatty acid binding site in subdomain II near Trp-214 and hydrophobic cavity of HSA.²⁴ It remains unclear if DPPC is quenching a single tryptophan on BSA or partially quenching both. Previous studies have shown higher numbers ($n = 1.76$) of 1,2-dioleoyl-*sn*-glycero-3-phosphoethanolamine (DOPE) binding to human serum albumin than to BSA ($n = 1.02$) utilizing similar techniques to those in this study. This difference was attributed by the authors to the differences in the quenching effect on Trp-214 in HSA in comparison to the partial quenching of each tryptophan in BSA.²⁰ These differences could be a result of significant differences between the two phospholipids with respect to the lipid headgroup (DPPC tertiary amine, DOPE primary amine) and acyl chain length and saturation (DPPC 16:0, DOPE 18:1).

The lack of notable shifts in $\lambda_{\text{em,max}}$ for all proteins suggest the quenching of intrinsic tryptophan fluorescence is most likely due to the aliphatic tails of the DPPC interacting with the hydrophobic domains of albumin which contain the tryptophan residues and not structural rearrangements resulting in changes

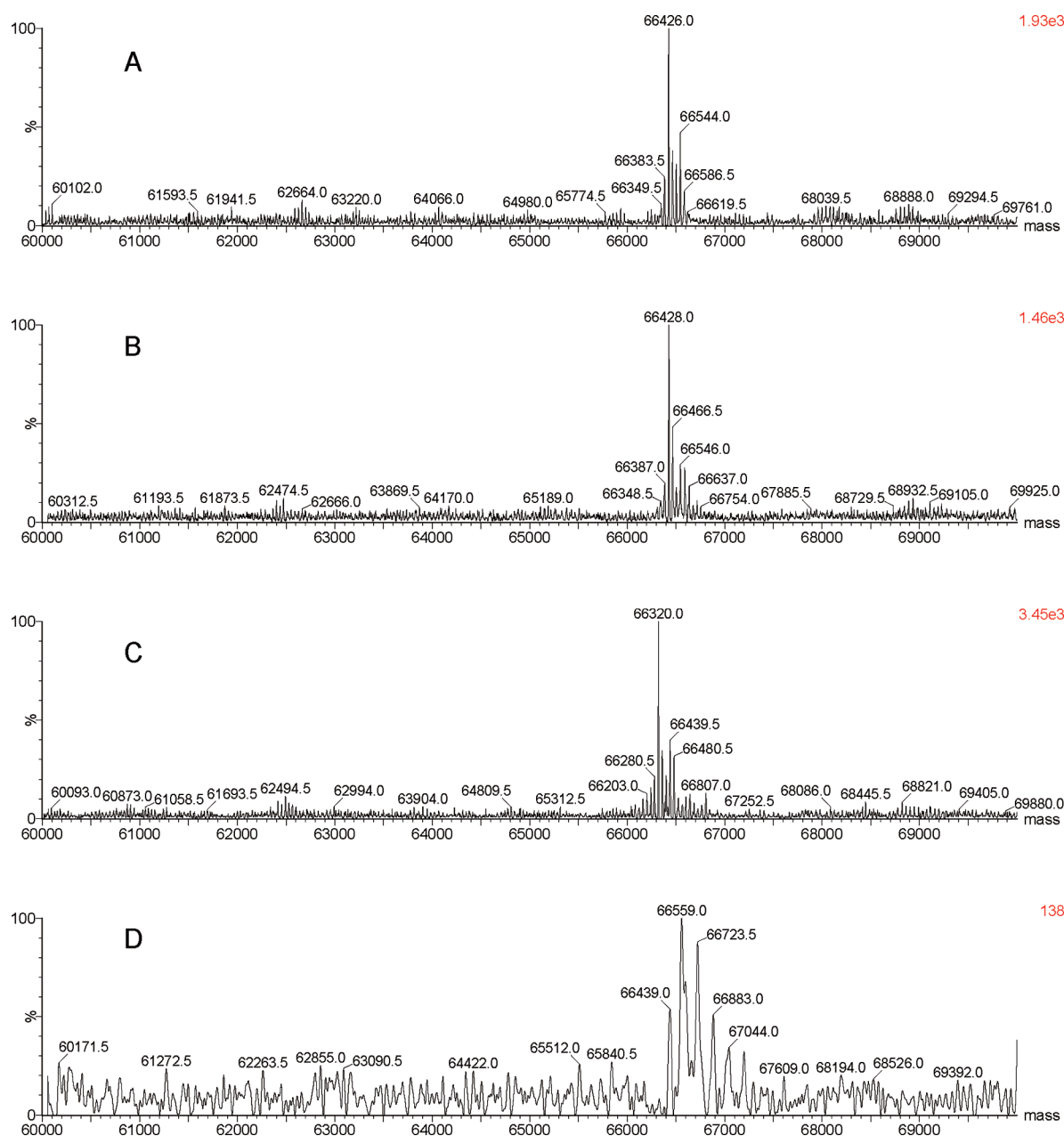


Figure 4. Deconvoluted intact mass spectra analysis of serum albumins samples. (A) BSA, (B) dfBSA, (C) PprHSA, (D) OsrHSA.

to the polarity of the solvent surrounding the tryptophan residues.^{19,20}

8-Anilino-1-naphthalene Sulfonic Acid (ANS) Fluorescence Analysis. ANS is a fluorescent probe that has an increased fluorescence intensity in hydrophobic environments, and this molecule has been used extensively to investigate protein structure and protein binding.³² OsrHSA and BSA showed reduced ANS fluorescence compared to PprHSA and dfBSA, respectively (Figure 7, Table 4). When liposomes were mixed with protein either prior to, or after, the addition of ANS, all albumins showed a striking decrease in ANS fluorescence intensity (Table 4). These results suggest that lipids from the liposome are competing for ANS binding sites, an idea which is supported by previous research showing that ANS and fatty acids compete for the same hydrophobic binding sites.³³ The reduced initial fluorescence intensity of free OsrHSA mixed with ANS compared to that of free PprHSA

suggests that fatty acids or lipids may already be present on OsrHSA.

DISCUSSION

This study demonstrates that 1,2-dipalmitoyl-*sn*-glycero-3-phosphocholine (DPPC) liposomes alter thermal stability of the secondary structure of HSA produced in *O. sativa* (OsrHSA), but not of HSA produced in *P. pastoris* (PprHSA). There are two major points of interest. The first concerns the mechanism that leads to different thermal stabilities being observed between the two recombinant HSA proteins. The second involves the mechanism by which DPPC liposomes alter the thermal stability of OsrHSA but not of PprHSA.

Similarities between BSA and OsrHSA were observed when comparing the biophysical properties of these two proteins to those of dfBSA and PprHSA, respectively. BSA and HSA share approximately 80% sequence homology, with most differences

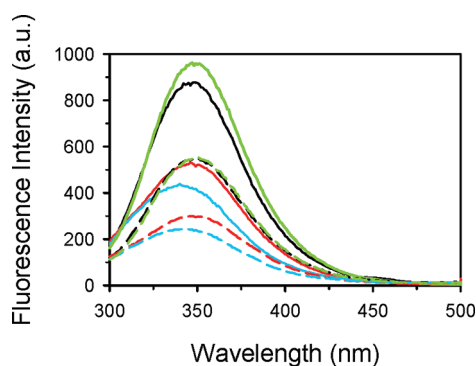


Figure 5. Representative intrinsic fluorescence emission spectra ($\lambda_{\text{ex}} = 280$ nm) of at least three separate experiments for four albumin samples in the absence (solid line) and presence (dashed line) of DPPC liposomes (200:1 total lipid/protein mol/mol) in buffer (5 mM NaPO_4 , pH 7.4) at 25 °C measured on a Varian Cary Eclipse Fluorescence Spectrometer. BSA (black plot), dfBSA (green plot), PprHSA (red plot), and OsrHSA (blue plot).

unlikely to affect protein structure, that is, hydrophobic residues for hydrophobic residues.³⁴ As such, a comparison between the bovine and recombinant human serum albumins studied here should give insight into the mechanism responsible for the observed differences in thermal stability between OsrHSA and PprHSA and the effect of DPPC liposomes. There are two possibilities that explain the differences in thermal stability between the two recombinant HSA proteins analyzed here. The first is the presence of lipid or fatty acids in greater number or in different composition on OsrHSA compared to PprHSA. The second is the presence of increased numbers of hexose glycation modifications on OsrHSA compared to PprHSA.

Studies presented here with BSA and dfBSA, as well as numerous other research reports, clearly show that the presence of fatty acids and/or surfactants improve the stability of albumin against thermal or chemical denaturation.^{35–38} For instance, studies by Shrake and co-workers demonstrate that the addition of six- and seven-carbon *n*-alkyl fatty acid anions increase the thermal stability of fatty acid-free human serum albumin by over 20 °C when measured with differential scanning calorimetry.³⁶ It is believed that the fatty acids provide a linkage between hydrophobic regions of a protein and positively charged amino acid residues, thereby stabilizing protein structure.³⁵

BSA demonstrates a reduction in maximal intrinsic fluorescence intensity, reduced ANS fluorescence, and an

increase in secondary structure thermal stability when compared to dfBSA. Similar trends were observed when OsrHSA was compared to PprHSA. Additionally, OsrHSA showed a blue shift in the $\lambda_{\text{em,max}}$ for intrinsic tryptophan fluorescence compared to PprHSA. The presence of fatty acids and phospholipids has been shown to blue shift and reduce the intensity of intrinsic tryptophan fluorescence in albumin.^{19,31,39}

The association of fatty acids with albumin has also been shown to reduce ANS fluorescence through competition with ANS for hydrophobic binding sites on the proteins.³³ Taken together, these observations support the hypothesis that fatty acids or lipids associated with OsrHSA are responsible for the improved thermal stability of this recombinant protein when compared to PprHSA.

Vetter and Indurthi and others have noted that glucose and glyoxylic acid glycation of serum albumin can also improve thermal stability.^{34,40} The presence of hexose glycation sites in greater numbers on OsrHSA, as detected through tandem MS, warrants further discussion.

Glycation of recombinant human serum albumin has been shown to change the secondary and tertiary structure as measured by far- and near-UV CD spectropolarimetry and intrinsic tryptophan fluorescence.^{34,40,41} It is believed that glycation results in local unfolding and a partial opening of hydrophobic pockets between domains,^{34,42} leading to higher content of β -sheet structure.³⁴ This in turn disrupts the unfolding pathway, resulting in more stable intermediates.^{34,42} When comparing PprHSA to OsrHSA, a number of observations suggest that the extensive hexose glycation of OsrHSA may be responsible for the improved secondary structure thermal stability. Via intrinsic tryptophan fluorescence studies, a blue-shifted $\lambda_{\text{em,max}}$ for OsrHSA was observed compared to PprHSA, as were minor changes to α -helical secondary structure, although no differences in tertiary structure were seen. Additionally, reduced ANS fluorescence was also observed for OsrHSA, which is expected with extensive glucose glycation of the protein.³⁴ However, similar increases in thermal stability were not observed for dfBSA relative to BSA despite the higher number of hexose glycation sites detected for dfBSA (seven versus three). This lack of correlation between the number of glycation sites for BSA/dfBSA and the thermal stability of the bovine serum albumins suggests that a minimum level of hexose glycation may be required for improved thermal stability (OsrHSA had more than twice as many glycation sites as dfBSA) or that hexose

Table 4. Summary of Fluorescence Data for the Four Serum Albumin Samples

sample	intrinsic fluorescence au maximum ^a	intrinsic fluorescence $\lambda_{\text{em,max}}$ (nm) ^a	ANS au maximum ^b	loss in ANS fluorescence intensity ^c	ANS $\lambda_{\text{em,max}}$ (nm) ^b
BSA	878.1 \pm 15.7	347.2 \pm 1.5	716.8 \pm 40.1	23%	472.3 \pm 1.3
BSA + DPPC liposomes	558.0 \pm 16.6	348.0 \pm 1.7	552.1 \pm 8.3		472.7 \pm 0.8
dfBSA	957.7 \pm 23.1	348.3 \pm 1.2	834.3 \pm 7.4	29%	473.5 \pm 1.2
dfBSA + DPPC liposomes	577.4 \pm 44.1	348.5 \pm 1.0	593.5 \pm 7.8		473.0 \pm 0.9
PprHSA	522.6 \pm 6.8	347.3 \pm 2.3	754.2 \pm 44.6	27%	473.7 \pm 1.4
PprHSA + DPPC liposomes	316.0 \pm 25.5	347.4 \pm 1.8	552.8 \pm 13.6		474.0 \pm 1.5
OsrHSA	439.5 \pm 11.1	340.2 \pm 1.6	509.8 \pm 4.1	15%	472.8 \pm 1.2
OsrHSA + DPPC liposomes	256.5 \pm 21.2	342.4 \pm 1.9	434.1 \pm 4.5		472.2 \pm 1.3

^aMean values \pm standard deviation for at least 5 separate experiments (calculated from Figure 5). ^bMean values \pm standard deviation for at least 3 separate experiments (calculated from Figure 7). ^cIn the presence of DPPC liposomes.

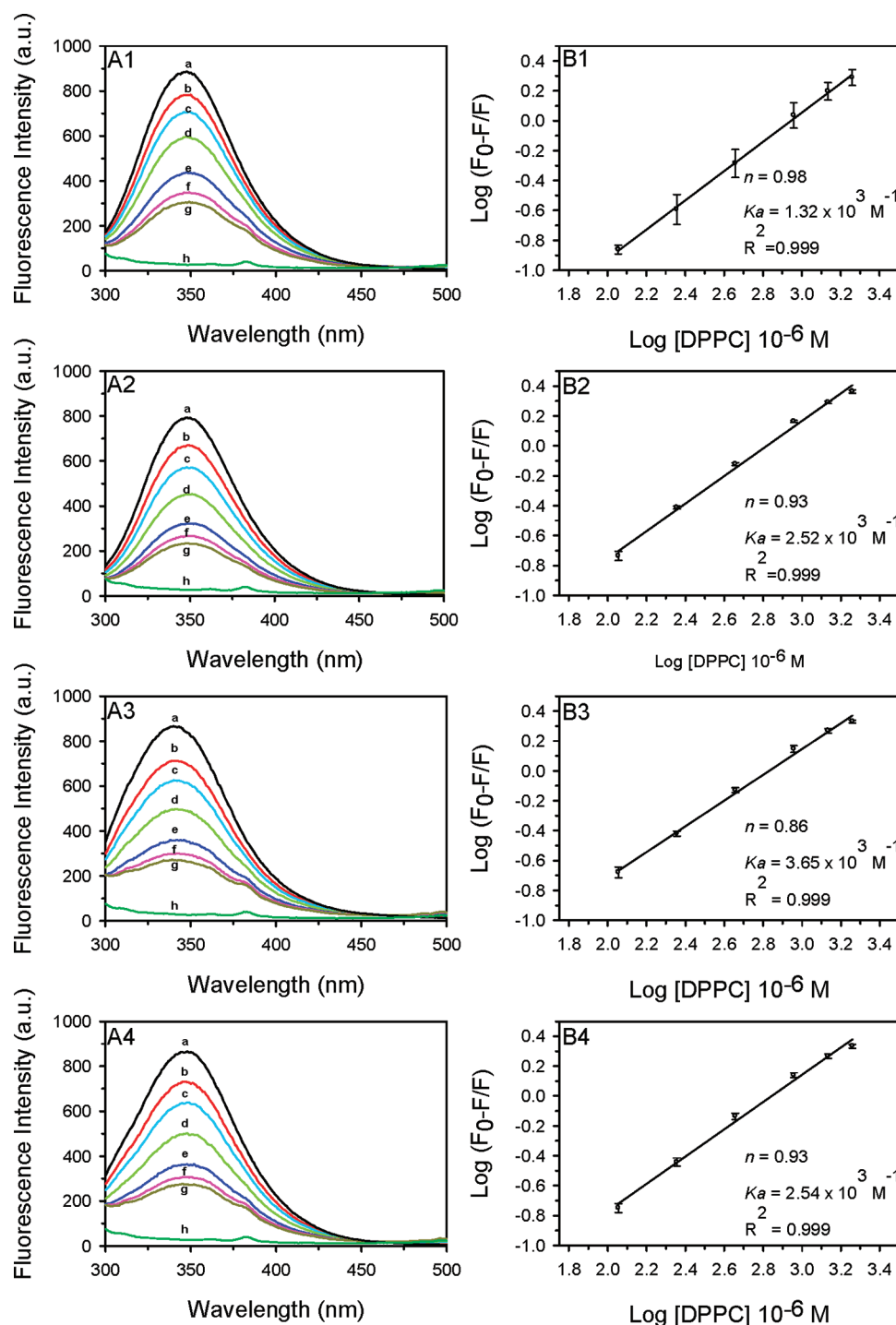


Figure 6. (A) Normalized fluorescence emission spectra for four serum albumin in increasing quantities of DPPC liposomes (total lipid/protein mol/mol) (5 mM NaPO_4 , pH 7.4). A1, BSA; A2, dfBSA; A3, OsrHSA; A4, PprHSA. (a) Black plots, free protein; (b) red plot, 50:1; (c) blue, 100:1; (d) olive, 200:1; (e) dark blue, 400:1; (f) pink, 600:1; (g) brown, 800:1; (h) green, liposome control. (B) Plots of $\log[F_0 - F/F]$ as a function of $\log[\text{DPPC}]$ for four serum albumins with calculated n and K_a values. B1, BSA; B2, dfBSA; B3, OsrHSA; B4, PprHSA.

glycation may not be responsible for the differing thermal stabilities of OsrHSA and PprHSA.

The second point of interest concerns the mechanism by which DPPC liposomes dramatically disrupt the secondary structure stability of OsrHSA but not PprHSA. Previous studies have shown that liposomes can affect the thermal stability of albumin^{5,9} and our studies confirmed this. In the presence of DPPC liposomes, OsrHSA appears to undergo subtle tertiary structural rearrangements as demonstrated by the changes to

the protein's near-UV spectropolarogram. These changes in tertiary structure correlate well with the observed reduction in OsrHSA secondary structure thermal stability evidenced by the loss of α -helical content. The two mechanisms which have been proposed to explain the differences in secondary structure thermal stability between OsrHSA and PprHSA may also explain how DPPC liposomes reduce the secondary structure stability of OsrHSA but not PprHSA.

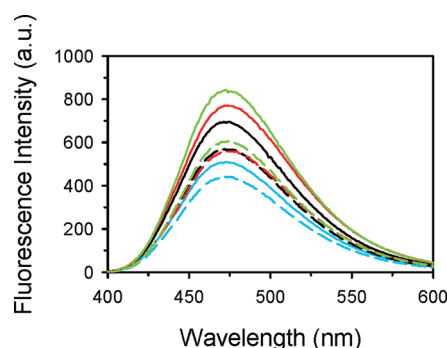


Figure 7. Representative 8-anilino-1-naphthalene sulfonic acid fluorescence emission spectra ($\lambda_{\text{ex}} = 380$ nm) of at least 3 separate experiments for four albumin samples in the absence (solid line) and presence (dashed line) of DPPC liposomes (200:1 total lipid/protein mol/mol) in buffer (5 mM NaPO₄, pH 7.4) at 25 °C measured on a Varian Cary Eclipse Fluorescence Spectrometer. BSA (black plot), dfBSA (green plot), PprHSA (red plot), and OsrHSA (blue plot).

The presence of lipid membranes may disrupt the native fatty acid–protein interactions that stabilize the structure of OsrHSA. Previous studies have shown that fatty acids noncovalently and reversibly bind to albumin and can undergo spontaneous transfer to lipid membranes.^{43,44} DPPC liposomes may remove fatty acids that are stabilizing the protein or replace anionic fatty acids with neutrally charged lipids that cannot bridge hydrophobic regions and cationic residues. This removal/exchange would eliminate the linkage between hydrophobic regions and positively charged amino acid residues resulting in the reduction of the thermal stability for the serum albumin. The observed changes in tertiary structure with OsrHSA in the presence of DPPC liposomes at 25 °C may be a result of these lipid/fatty acid exchanges allowing for greater movement of secondary structural elements and domains. Further supporting this proposed mechanism is a correlation of BSA/dfBSA data with OsrHSA/PprHSA observations. Similar to OsrHSA, BSA (which contains fatty acids), in the presence of DPPC liposomes has reduced secondary structure thermal stability and a smaller decrease in ANS fluorescence relative to dfBSA.

Alternatively, the presence of extensive hexose glycation detected on OsrHSA may result in structural changes that generate novel fatty acid binding sites.³⁴ These novel binding sites and the opening of hydrophobic pockets may allow lipids from DPPC liposomes to disrupt local side chain interactions (secondary structure) or nonlocal interactions (tertiary structure), both of which have been shown to affect protein structure stability.^{45,46} Both OsrHSA and dfBSA demonstrated changes in tertiary structure in the presence of DPPC; however, no correlation was observed between DPPC liposome-induced thermal stability reduction and hexose glycation for dfBSA. Again this suggests that a minimal number of hexose glycation sites may be required for DPPC liposomes to reduce structural stability or that hexose glycation is not playing a role in the reduction of OsrHSA stability by these particles.

CONCLUSIONS

We have shown that DPPC liposomes can dramatically alter the thermal stability of human serum albumin expressed in *O. sativa*, but not of that expressed in *P. pastoris*. We have presented, in our view, two plausible mechanisms for these observations that are supported by our experimental data. Our

future research will be focused on elucidating the mechanism by which DPPC liposomes reduce the thermal stability of HSA produced in *O. sativa* but not *P. pastoris*. An obvious approach would be to remove the fatty acids or lipids bound to BSA, and putatively OsrHSA, and to reassess the secondary structure thermal stability of each protein in the presence of DPPC liposomes. Although a number of techniques have been published to accomplish this, the challenge is to ensure the native structure of the protein remains intact after lipid removal.⁴⁷ Many of these techniques utilize low pH (<3.0) for extended periods of time and/or organic solvents⁴⁷ which could result in structural rearrangements or protein aggregation,⁴⁸ potentially leading to changes in thermal stability unrelated to the presence of lipids or fatty acids.

Regardless of the mechanism(s) involved, we believe this study will have an impact on protein–nanoparticle research. Numerous studies have utilized albumin from various sources to evaluate the interaction of nanoparticles and plasma proteins. We have shown that recombinant proteins with identical amino acid sequences (with the exception that the first Asp, which is considered non structural, is deleted in PprHSA) and similar secondary and tertiary structures have widely different interactions with liposomes. We believe that future protein–nanoparticle studies involving albumin or other recombinant proteins will require additional focus placed on the expression system and any post-translational modifications that are present.

AUTHOR INFORMATION

Corresponding Author

*E-mail: michael.johnston@hc-sc.gc.ca. Fax: (613) 941-8933
Phone: (613) 941-1540.

Notes

The authors declare no competing financial interest.

ACKNOWLEDGMENTS

This research is supported by the Government of Canada. We would like to thank Drs. Mary Alice Hefford and Aaron Farnsworth for their critical review of this manuscript.

REFERENCES

- (1) Allen, T. M.; Cullis, P. R. *Science* **2004**, *303*, 1818–1822.
- (2) Hofheinz, R. D.; Gnad-Vogt, S. U.; Beyer, U.; Hochhaus, A. *Anticancer Drugs* **2005**, *16*, 691–707.
- (3) Balasubramanian, S. V.; Bruenn, J.; Straubinger, R. M. *Pharm. Res.* **2000**, *17*, 344–350.
- (4) Sivan, S.; Schroeder, A.; Verberne, G.; Merker, Y.; Diminsky, D.; Prie, A.; Maroudas, A.; Halperin, G.; Nitzan, D.; Etsion, I.; et al. *Langmuir* **2010**, *26*, 1107–1116.
- (5) Sabin, J.; Prieto, G.; Ruso, J. M.; Messina, P. V.; Salgado, F. J.; Nogueira, M.; Costas, M.; Sarmiento, F. *J. Phys. Chem. B* **2009**, *113*, 1655–1661.
- (6) Chonn, A.; Semple, S. C.; Cullis, P. R. *J. Biol. Chem.* **1992**, *267*, 18759–18765.
- (7) Hernandez-Caselles, T.; Villalain, J.; Gomez-Fernandez, J. C. *Mol. Cell. Biochem.* **1993**, *120*, 119–126.
- (8) Dimitrova, M. N.; Matsumura, H.; Dimitrova, A.; Neitchev, V. Z. *Int. J. Biol. Macromol.* **2000**, *27*, 187–194.
- (9) Pantusa, M.; Sportelli, L.; Bartucci, R. *Eur. Biophys. J.* **2008**, *37*, 961–973.
- (10) Galantai, R.; Bardos-Nagy, I. *Int. J. Pharm.* **2000**, *195*, 207–218.
- (11) Ruiz, L.; Reyes, N.; Duany, L.; Franco, A.; Aroche, K.; Hardy, R. E. *Int. J. Pharm.* **2003**, *264*, 57–72.

- (12) Petrelli, F.; Borgonovo, K.; Barni, S. *Expert Opin. Pharmacother.* **2010**, *11*, 1413–1432.
- (13) Quinlan, G. J.; Martin, G. S.; Evans, T. W. *Hepatology* **2005**, *41*, 1211–1219.
- (14) Mandeville, J. S.; Tajmir-Riahi, H. A. *Biomacromolecules* **2010**, *11*, 465–472.
- (15) Worn, A.; uf der, M. A.; Escher, D.; Honegger, A.; Barberis, A.; Pluckthun, A. *J. Biol. Chem.* **2000**, *275*, 2795–2803.
- (16) Di, N. L.; Whitson, L. J.; Cao, X.; Hart, P. J.; Levine, R. L. *J. Biol. Chem.* **2005**, *280*, 39907–39913.
- (17) Willuda, J.; Honegger, A.; Waibel, R.; Schubiger, P. A.; Stahel, R.; Zangemeister-Wittke, U.; Pluckthun, A. *Cancer Res.* **1999**, *59*, 5758–5767.
- (18) Cha, S. S.; Kim, J. S.; Cho, H. S.; Shin, N. K.; Jeong, W.; Shin, H. C.; Kim, Y. J.; Hahn, J. H.; Oh, B. H. *J. Biol. Chem.* **1998**, *273*, 2153–2160.
- (19) Charbonneau, D.; Beauregard, M.; Tajmir-Riahi, H. A. *J. Phys. Chem. B* **2009**, *113*, 1777–1784.
- (20) Charbonneau, D. M.; Tajmir-Riahi, H. A. *J. Phys. Chem. B* **2010**, *114*, 1148–1155.
- (21) Kobayashi, K. *Biologicals* **2006**, *34*, 55–59.
- (22) Webster, D. E.; Thomas, M. C. *Biotechnol. Adv.* **2012**, *30*, 410–418.
- (23) Sugio, S.; Kashima, A.; Mochizuki, S.; Noda, M.; Kobayashi, K. *Protein Eng.* **1999**, *12*, 439–446.
- (24) He, Y.; Ning, T.; Xie, T.; Qiu, Q.; Zhang, L.; Sun, Y.; Jiang, D.; Fu, K.; Yin, F.; Zhang, W.; et al. *Proc. Natl. Acad. Sci. U.S.A* **2011**, *108*, 19078–19083.
- (25) Johnson, W. C. *Proteins* **1999**, *35*, 307–312.
- (26) Kinderlerer, J.; Lehmann, H.; Tipton, K. F. *Biochem. J.* **1973**, *135*, 805–814.
- (27) Digel, I.; Maggakis-Kelemen, C.; Zerlin, K. F.; Linder, P.; Kasischke, N.; Kayser, P.; Porst, D.; Temiz, A. A.; Artmann, G. M. *Biophys. J.* **2006**, *91*, 3014–3021.
- (28) Kelly, S. M.; Price, N. C. *Curr. Protein Pept. Sci.* **2000**, *1*, 349–384.
- (29) Kleinova, M.; Belgacem, O.; Pock, K.; Rizzi, A.; Buchacher, A.; Allmaier, G. *Rapid Commun. Mass Spectrom.* **2005**, *19*, 2965–2973.
- (30) Royer, C. A. *Chem. Rev.* **2006**, *106*, 1769–1784.
- (31) Lautenslager, G. T.; Shearman, C. W.; Hud, E.; Cohen, M. P. *Metabolism* **2011**, *60*, 1683–1691.
- (32) Trynda-Lemiesz, L.; Wiglusz, K. *J. Pharm. Biomed. Anal.* **2010**, *52*, 300–304.
- (33) Takehara, K.; Yuki, K.; Shirasawa, M.; Yamasaki, S.; Yamada, S. *Anal. Sci.* **2009**, *25*, 115–120.
- (34) Rondeau, P.; Bourdon, E. *Biochimie* **2011**, *93*, 645–658.
- (35) Moriyama, Y.; Watanabe, E.; Kobayashi, K.; Harano, H.; Inui, E.; Takeda, K. *J. Phys. Chem. B* **2008**, *112*, 16585–16589.
- (36) Shrake, A.; Frazier, D.; Schwarz, F. P. *Biopolymers* **2006**, *81*, 235–248.
- (37) Leggio, C.; Galantini, L.; Konarev, P. V.; Pavel, N. V. *J. Phys. Chem. B* **2009**, *113*, 12590–12602.
- (38) Moriyama, Y.; Kawasaka, Y.; Takeda, K. *J. Colloid Interface Sci.* **2003**, *257*, 41–46.
- (39) Spector, A. A.; John, K. M. *Arch. Biochem. Biophys.* **1968**, *127*, 65–71.
- (40) Vetter, S. W.; Indurthi, V. S. *Clin. Chim. Acta* **2011**, *412*, 2015–2116.
- (41) Nakajou, K.; Watanabe, H.; Kragh-Hansen, U.; Maruyama, T.; Otagiri, M. *Biochim. Biophys. Acta* **2003**, *1623*, 88–97.
- (42) Mendez, D. L.; Jensen, R. A.; McElroy, L. A.; Pena, J. M.; Esquerra, R. M. *Arch. Biochem. Biophys.* **2005**, *444*, 92–99.
- (43) Abreu, M. S.; Estronca, L. M.; Moreno, M. J.; Vaz, W. L. *Biophys. J.* **2003**, *84*, 386–399.
- (44) Pantusa, M.; Sportelli, L.; Bartucci, R. *Biophys. Chem.* **2005**, *114*, 121–127.
- (45) Kragh-Hansen, U.; Watanabe, H.; Nakajou, K.; Iwao, Y.; Otagiri, M. *J. Mol. Biol.* **2006**, *363*, 702–712.
- (46) Munoz, V.; Cronet, P.; Lopez-Hernandez, E.; Serrano, L. *Folding Des.* **1996**, *1*, 167–178.
- (47) Chen, R. F. *J. Biol. Chem.* **1967**, *242*, 173–181.
- (48) Bhattacharya, M.; Jain, N.; Bhasne, K.; Kumari, V.; Mukhopadhyay, S. *J. Fluoresc.* **2011**, *21*, 1083–1090.